Rui Li[a], Wenguo Wang[a], Fosheng Li, Qingwei Wang, Shenghua Wang, Ying Xu* and Fang Chen

Response of alternative splice isoforms of *OsRad9* gene from *Oryza sativa* to environmental stress

DOI 10.1515/znc-2016-0257
Received December 28, 2016; revised January 4, 2017; accepted February 11, 2017

Abstract: *Rad9* protein plays an important role in cell-cycle checkpoint signal transduction in human and yeast cells, but knowledge about *Rad9* in plants is limited. This study reports that the *Rad9* gene of rice can generate the transcript products *OsRad9.1* and *OsRad9.2* through alternative splicing. *OsRad9.1*, with all nine exons, is the main cell-cycle checkpoint protein involved in the response of rice to genotoxic stresses (ultraviolet radiation and antibiotic stress), environmental stresses (drought, salt, and heavy metal stress), and auxin stimuli (2,4-D, IAA, and IBA). Meanwhile, transcript isoform *OsRad9.2*, which lost exon7 and exon8, showed different preferential stimulation effects on these stresses and pollen development duration. These results might indicat that besides the monitoring and repair of DNA damage, *Rad9* might involve in the development of pollen.

Keywords: abiotic stress; alternative splicing; auxin; gene expression; *Rad9*.

1 Introduction

DNA damage induced by stresses [e.g. ionizing radiation, ultraviolet (UV) radiation, chemical mutagens, metabolic byproducts, and stalled replication forks] is a relatively common event in the life of a cell [1]. In response to DNA damage, organisms have evolved various defense mechanisms to eliminate or reduce these stresses. One such defense mechanism is the cell-cycle checkpoint control system. This system uses a number of DNA damage sensor proteins to detect damaged or abnormally structured DNA and further activate a series of downstream signal pathways to repair damaged DNA or apoptosis to maintain genomic stability [2, 3].

Rad9 is a key component of the checkpoint signaling pathway and constitutes a heterotrimeric complex (the 9-1-1 complex) with *Hus1* and *Rad1* [4]. When DNA damage is detected, the 9-1-1 complex is loaded onto the site of DNA damage and then coordinates checkpoint activation and DNA repair [5, 6]. *Rad9* has two structural domains. One is proliferating cell nuclear antigen (PCNA)–like binding motif in the N-terminal of *Rad9*, which is associated with *Hus1* and *Rad1* to form the 9-1-1 complex [7]; the other is a tandem domain in its carboxyl terminus, which is heavily phosphorylated in response to cell cycle position and DNA damage [8–10]. In addition to its function in the 9-1-1 complex, *Rad9* also participates in immunoglobulin class switch recombination as a transcription factor and shows 3′–5′ exonuclease activity [11, 12]. Aberrant *Rad9* expression has been associated with prostate, breast, lung, skin, thyroid, and gastric cancers [13]. Hence, *Rad9* has multiple functions for preserving genomic integrity.

However, these studies on *Rad9* mechanisms have been mainly conducted in animals and yeast, and studies on *Rad9* in plants are few. A paper on *Arabidopsis* showed that *AtRad9* mutants exhibit extreme sensitivity to DNA-damaging chemicals and have similar phenotypes to those of mutants for the corresponding human gene, thus suggesting a similarity in plant and animal's cell checkpoint function [14]. In this paper, we identified and characterized the *OsRad9* gene of rice. *OsRad9* generated the proteins *OsRad9.1* and *OsRad9.2*, by alternative splicing of the transcript. *OsRad9.1*, as the cell-cycle checkpoint protein, was highly expressed in almost all tissues examined, whereas *OsRad9.2* gave a high level of expression in developmental pollen. Thus, *OsRad9* may have multiple functions in rice development process.

[a]Rui Li and Wenguo Wang authors contributed equally to this work
***Corresponding author: Ying Xu,** Key Lab of Bio-Resources and Eco-Environment, Ministry of Education, College of Life Science, Sichuan University, Chengdu 610064, China, Tel.: +86 28 85417281, Fax: 86 028 85417281, E-mail: xuying@scu.edu.cn
Rui Li: College of Pharmacy and Biological Engineering, Chengdu University, 1 Shiling, Chengdu 610106, China
Wenguo Wang: Biogas Institute of Ministry of Agriculture, Chengdu 610041, China
Fosheng Li, Qingwei Wang, Shenghua Wang and Fang Chen: Key Lab of Bio-Resources and Eco-Environment, Ministry of Education, College of Life Science, Sichuan University, Chengdu 610064, China

2 Materials and methods

2.1 Plant material, growth condition, and treatments

Seeds of rice (*Oryza sativa* L.) Zhonghua 11 and male sterile line m393LA were grown in a natural environment on a farmland in Chendu City (Sichuan Province, China). Samples of root, stem, leaf, abortion, unicellular pollen, bicellular pollen, and tricellular pollen were collected and stored at −80 °C. The isolation and purification of developmental pollen were conducted according to the method described by Peng et al. [15].

Stress treatments included genotoxic stress, UV radiation, antibiotic agents such as bleomycin and mitomycin C (MMC), and environmental stresses such as drought, salt (NaCl), $CdCl_2$, and $HgCl_2$ stress. Ten-day-old seedlings were exposed to UV rays at 240 lm for 1, 2, 5, or 10 h. The wavelength of UV rays was 253.7 nm (wavelength region, 220–300 nm), which is mostly used in biological studies. Antibiotic stress assays were performed as previously described by Heitzeberg et al. [14]. Approximately 1 cm-tall seedlings grown in darkness were incubated in MS medium containing 1 µg/mL bleomycin or 40 µg/mL MMC. For environmental stress treatments, 1-month-old seedlings were treated with 0.2 M NaCl, 0.5 M $CdCl_2$, and 0.5 M $HgCl_2$, respectively, whereas drought stress was induced by natural drying instead of watering the solution.

To study the expression pattern of *Rad9* response to auxin in the context of rice callus formation, rice callus induction assays were conducted as described by Luo et al. [16]. After surface sterilizing with 75% ethanol and 1.5% sodium hypochlorite and then washing three times with sterile water, seeds were inoculated on MS medium supplemented with different auxin sources [2,4-D, Indole-3-acetic acid (IAA), and Indole-3-Butytric acid (IBA)] and subsequently cultured in darkness. Auxin concentrations were 0.5, 1.0, 2.0, and 5.0 mg/L.

All harvested materials were immediately frozen in liquid nitrogen and then stored at −80 °C for RNA preparation. At least three independent replicates of each experiment were performed.

2.2 Amplification and sequence analysis of *OsRad9* gene

Total RNA of rice samples was extracted using Trizol reagent (Invitrogen, Carlsbad, CA, USA). Reverse transcription of pooled RNA was carried out with oligodeoxythymidine using the PrimeScript™ RT Reagent Kit (TaKaRa, Dalian, China) according to the manufacturer's instructions. PCR primers (Table 1) were designed based on the sequence from the Rice Genome Annotation Project (http://rice.plantbiology.msu.edu/, LOC_Os03g22450). PCR reaction was conducted as described previously by Wang et al. [17].

After identifying on 1% agarose gels, PCR products were cloned into the pMD19-T vector (Takara, Dalian, China) and sequenced. Sequence similarities were examined with the GenBank/EMBL database using the BLAST program (http://blast.ncbi.nlm.nih.gov/Blast.cgi). The amino acid sequences of cloned cDNA fragments were deduced and protein sequences were aligned using the program DNAMAN 6.0 (http://www.lynnon.com). Phylogenetic relationship was analyzed by multiple alignments of *Rad9* proteins using the MEGA 4.1 program and visualized by iTOL (http://itol.embl.de/) [18].

2.3 Location assays of *OsRad9*-GFP-Fusion proteins

Transient expression assays in onion epidermal cells were carried out by *Agrobacterium* mediated transformation. cDNAs of *OsRad9.1* and *OsRad9.2* were linked to the 5′ end of *gfp* gene and then inserted to multiple cloning sites of pBI221 vector to make fusion gene expression vectors. *Agrobacterium* transformation was conducted as described by Li et al. [19]. A small piece (~1 cm^2) of onion epidermis was torn off under sterile conditions and

Table 1: Primers for PCR used in this paper.

Primers	Sequences	Usage
Rad9-F	5′-ATGGAGCTGTCTATGAGCGG-3′	Cloning of *OsRad9* cDNA
Rad9-R	5′-CTAGTCCATGTAGTGCGGTG-3′	Cloning of *OsRad9* cDNA
Rq1F:	5′-TGGAAGAGCCTCCTGATGTTG-3′	Quantitative Real-time PCR
Rq2F:	5′-GGTCGGAGCTATCAGATGTTG-3′	Quantitative Real-time PCR
Rq-R:	5′-ATGTAGTGCGGTGTTGTTTGG-3′	Quantitative Real-time PCR
*actin*_f:	5′-GACTCTGGTGATGGTGTCAGC-3′	Quantitative Real-time PCR
*actin*_r:	5′-GGCTGGAAGAGGACCTCAGG-3′	Quantitative Real-time PCR

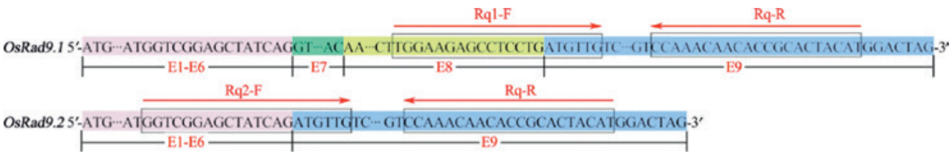

Figure 1: Exon-structure diagram of the two mRNA isoforms of *OsRad9*. The location of the primers is shown in the box. Rq1-F is located beteewn exon8 and 9 junctions, Rq2-F is located beteewn exon6 and 9 junctionsis, Rq-R is located downstream of the exon9.

infected with *Agrobacterium* suspension for 20 min. After bacterial liquids were absorbed with filter paper, the flake was placed on MS medium and cocultured for 24 h at 25 °C and 16 h light/8 h darkness. After cleaning the bacteria with sterile liquid MS medium, cell layers were mounted in water and examined by epifluorescence microscopy (Olympus SZX2-ILLB, Japan) with a GFP2 filter (480 nm excitation filter/510 nm barrier filter).

2.4 Real-time quantitative PCR analysis of *OsRad9* mRNA

Total RNA was extracted using the method described above. Approximately 0.5 µg of total RNA from each pool was reverse transcribed to cDNA with oligodeoxythymidine in a volume of 10 µL following the PrimeScript™ RT Reagent Kit protocol.

The synthesized cDNA was diluted to 100 µL with sterile water and used as template in real-time quantitative PCR (qRT-PCR). Gene-specific primers (Table 1) were designed using Primer 5.0 software (PREMIER Biosoft International, Palo Alto, CA, USA) to amplify the specific cDNA fragment of two isoforms, *OsRad9.1* and *OsRad9*.2. The two isoforms had same reverse primer but different forward primes (Table 1). As showed in Figure 1, the forward primer of isoform *OsRad9.1* (Rq1-F) includes 15 nt of the end of Exon 8 and 6 nt of the front of Exon 9. The forward primer of isoform *OsRad9.2* also includes the same 6 nt of the front of Exon 9, but the other 15 nt of the primer is from the end of Exon 6. All qRT–PCRs were performed using SYBR® Premix Ex Taq™II (TaKaRa, Dalian, China) and a Bio-Rad CFX96 Real-time PCR machine. Cycling parameters for *OsRad9* were 95 °C for 10 s initially, followed by 40 cycles, each comprising 95 °C for 10 s, 60 °C for 20 s and 72 °C for 20 s, then 3 min at 72 °C. *Os-actin* PCR conditions were 95 °C for 10 s initially, followed by 40 cycles, each comprising 95 °C for10 s, 63 °C for 20 s and 72 °C for 20 s, then 3 min at 72 °C.

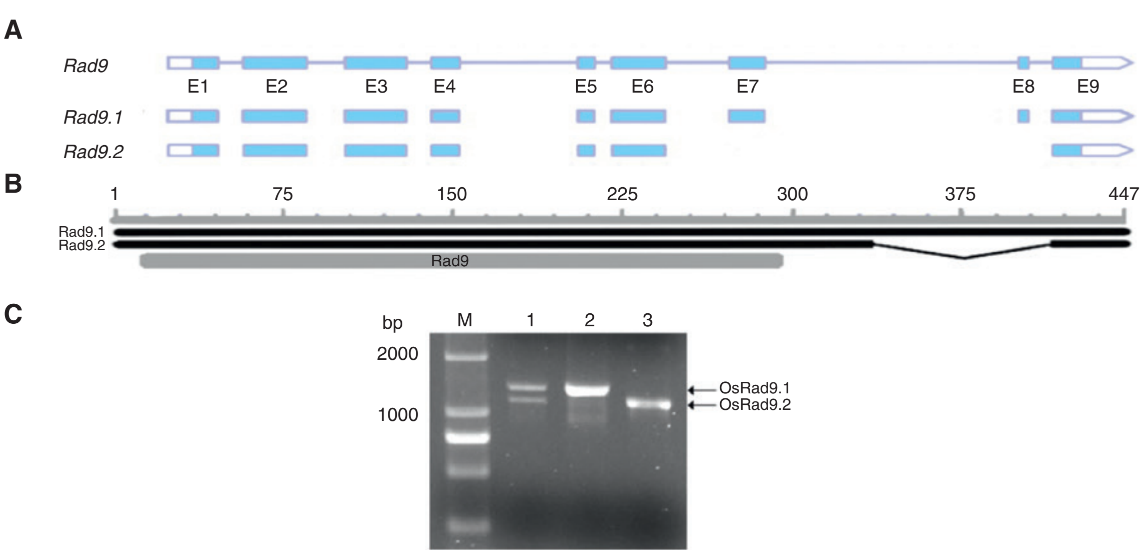

Figure 2: *OsRad9* gene structure and RT-PCR analysis. (A) Schematic depiction of the genomic structure of *OsRad9* and alternative splicing of the two transcript isoforms. Line above shows the genomic contig from genome database. The exons and introns are represented by boxes and lines, respectively. (B) BLASTP analysis of amino acid sequences of *OsRad9.1* and *OsRad9.2* in the GenBank. The polyline denotes alternative splicing region. The hatched box indicates a *Rad9* domain. (C) Detection of alternative transcripts of *OsRad9* by RT-PCR. Lane M, DNA molecular weight marker (bp); lane 1, PCR amplification from rice callus cDNA; lane 2 (*OsRad9.1*), lane 3 (*OsRad9.2*).

3 Results

3.1 Isolation and sequence analysis of *OsRad9*

According to the rice genome data (http://rice.plantbiology.msu.edu/), *OsRad9* gene was located on the long arm of chromosome 3 (Loc_Os03g22450) and contained nine exons forming an ORF of 1344 nucleotides coding for a putative protein of 447 aa (Figure 2A). The putative protein of *OsRad9* was homologous to ARF75 (AJ441077) of *Arabidopsis thaliana* in Genbank. However, we further found that the naming of AtARF75 was based on experimental evidence, no additional details recorded (http://www.ncbi.nlm.nih.gov/protein/CAD29645.1). And with no auxin response elements (AuxREs), the putative ARF75 do not in the ARF family of both rice and *Arabidopsis thaliana* [20]. When the putative amino acids of *OsRad9* were used for BLASTP, two records (EEC75240.1 and ABF95895.1) were found in GenBank, and both of them had completed *Rad9* domain (Figure 2B). Hence, our research focus was transferred to *Rad9* gene. Sequence analysis revealed that *OsRad9* protein shared conserved domains and that the difference between the two records mainly occurred in the C-terminal portion of *OsRad9* (Figure 2A and B). These analyses indicated that EEC75240.1 and ABF95895.1 were products alternatively spliced from *OsRad9* transcripts. For confirmation, we conducted reverse-transcriptase PCR (RT-PCR) analysis using total RNA from rice callus. As expected, two bands could be amplified (Figure 2C) and designated as *OsRad9.1* and *OsRad9.2*, corresponding

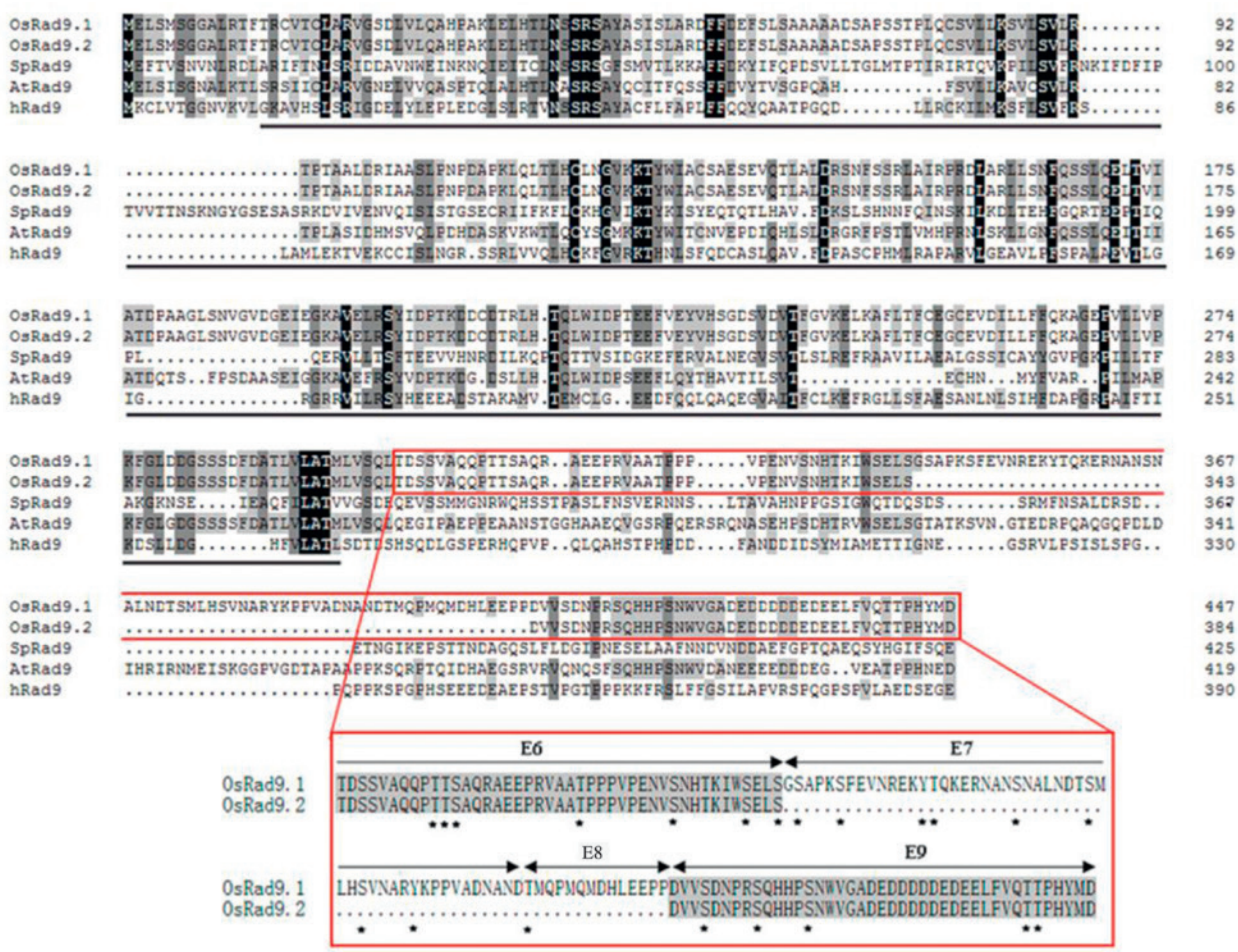

Figure 3: Multiple alignment of *Rad9* proteins from several species. The sequences for alignment from the published sequences of *Rad9s*, *SpRad9* (CAA46693.1) from *Schizosaccharomyces pombe*, *AtRad9* (NP_001030644.1) from *Arabidopsis thaliana* and *hRad9* (AAH14848.1) from *Homo sapiens*. Dark shadow amino acids indicate identity and light shadow amino acids indicate chemically similar amino acids. The continuous underline denotes the *Rad9* region. The C-terminal region is enclosed by the red box. The asterisk denotes potential phosphorylation sites.

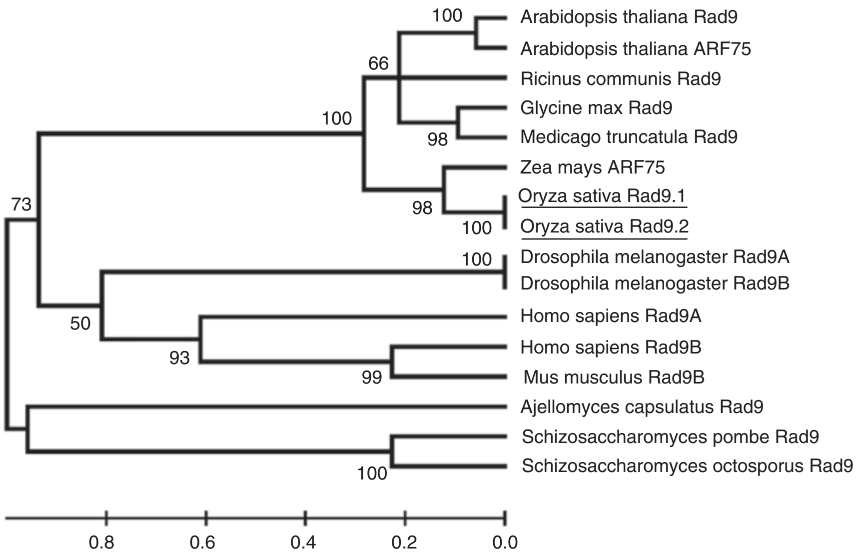

Figure 4: Phylogenetic tree of *Rad9* protein sequences from different species. The *OsRad9* proteins were shown continuous underline in picture.

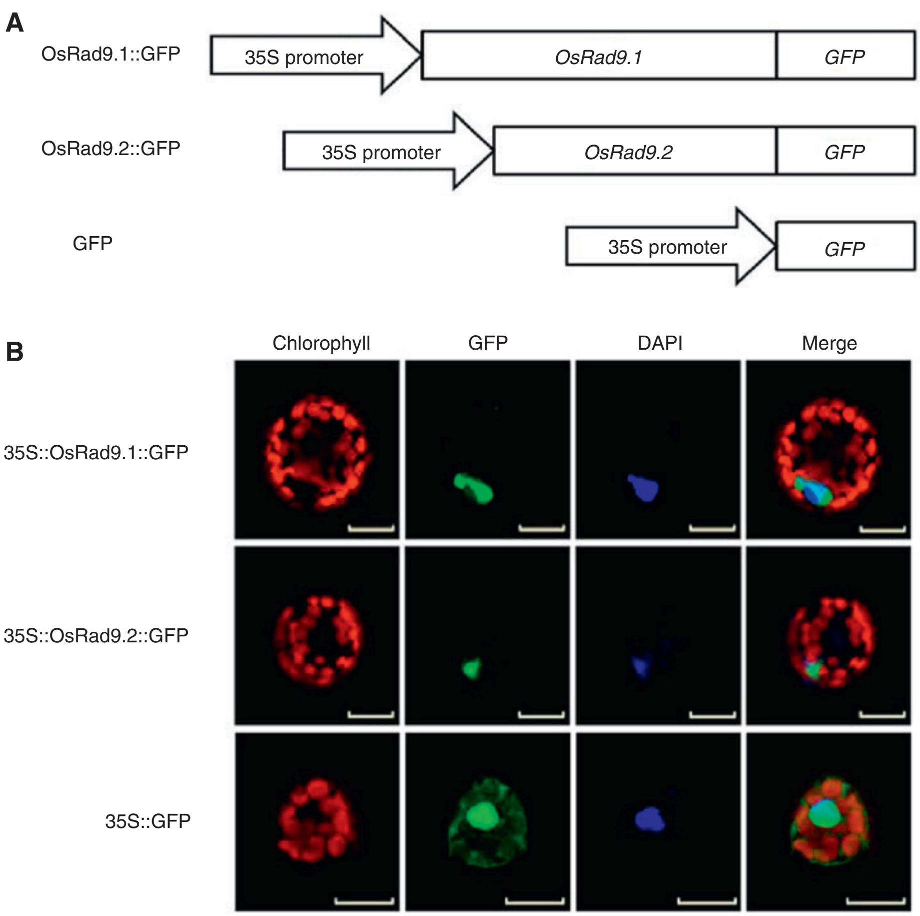

Figure 5: Subcellular localization of the two *OsRad9* transcript isoforms. (A) Schematic depiction of the *GFP*, *OsRad9.1::GFP* and *OsRad9.2::GFP* fusion constructs. The constitutive 35S CaMV promoter was used to express these fusion proteins in onion cells. (B) Subcellular localization of *OsRad9.1*::GFP and *OsRad9.2*::GFP. The fluorescent images of the GFP fusion proteins are shown in the left panels and the bright images of the GFP fusion proteins are shown in the right panels.

to EEC75240.1 and ABF95895.1, respectively. Further cloning, sequencing, and sequence comparison showed that *OsRad9* had very high similarity to *Rad9* from other species, especially in the N-terminal region of the encoded peptides. Some examples were as follows: 24.54% similarity to *hRad9*, 20.55% to *SpRad9*, and the closest homolog in the PCNA family that charged for the *Rad9–Hus1–Rad1* clamb complex. Thus, they can all act as DNA damage sensors and are loaded around DNA [21, 22].

C-terminal analysis using the web-based server KinasePhos [23] with default parameters showed that *OsRad9.1* contained 21 phosphorylation sites (amino acids 301–447), whereas *OsRad9.2* only had 12 phosphorylation sites (amino acids 301–384) with exon7 and exon8 missing (Figure 3).

Phylogenetic analysis showed that *Rad9* had obvious differentiation between animals and plants, with *OsRad9* transcript isoforms closely related to *ARF75* of monocot maize; plant *Rad9* homologs were divided into two main groups, dicotyledons and monocotyledons (Figure 4).

3.2 Subcellular localization of *OsRad9*

Rad9 proteins are reportedly localized to the cell nucleus [24–26]; thus, information on the subcellular localization of these proteins can help elucidate the functional roles that proteins play in cells. To analyze the localization patterns of *OsRad9.1* and *OsRad9.2*, we linked them to *GFP* for fusion proteins, and transient expression conducted in onion epidermal cells showed that *OsRad9.1* and *OsRad9.2* protein signals appeared only in the nucleus (Figure 5). This finding indicated that both *OsRad9.1* and *OsRad9.2* functioned in the nucleus and that genome DNA was their main target.

3.3 Spatial expression patterns of *OsRad9* transcript isoforms

The expression analysis of *OsRad9* based on RT-PCR and qRT-PCR showed that the two *OsRad9* transcript isoforms had different expression patterns (Figure 6). *OsRad9.1* was

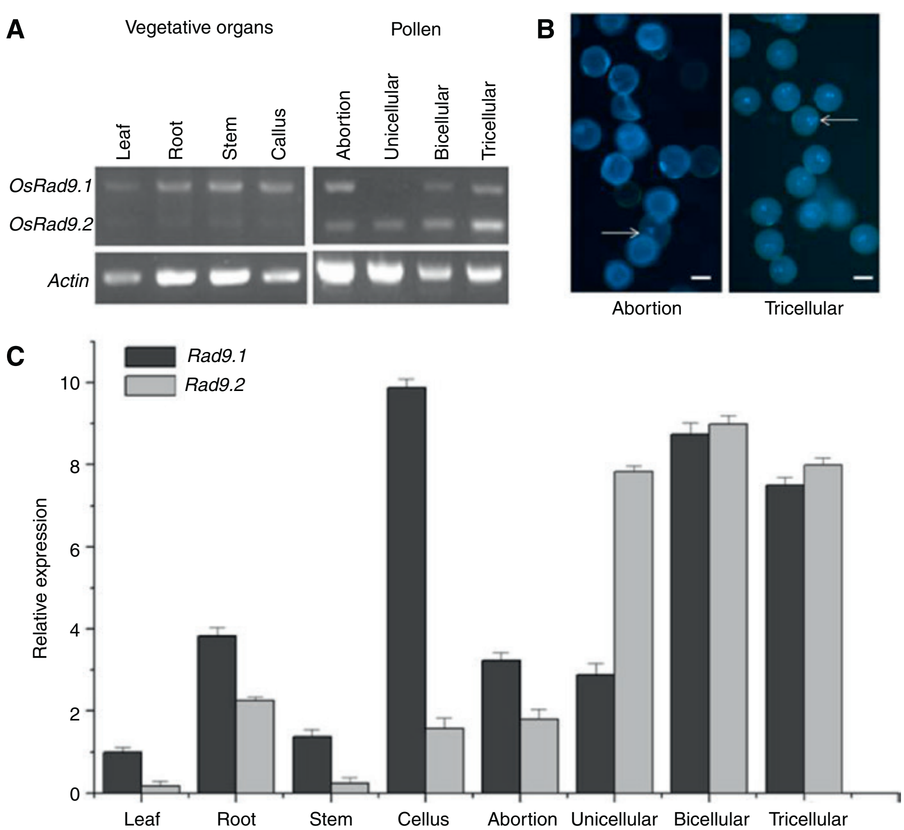

Figure 6: Spatial expression patterns of two *OsRad9* isoforms by RT-PCR (A) and qRT-PCR (C) in different tissues: leaf, root, stem, callus, abortion pollen, unicellular pollen, bicellular pollen and tricellular pollen, (B) Pollen grains were isolated from the tricellular stage of the male sterile line m393LA and Zhonghua 11 line, respectively, and examined by Dye 4′-6-diamidino-2-phenylindole (DAPI) staining, arrows denote the nucleus, bars: 20 μm.

expressed predominantly in root, stem, leaf, especially in callus (Figure 6A and C).

Meanwhile, *OsRad9.2* expression was much higher in pollen than somatic tissues (Figure 6A and C). In pollen development, the expression of *OsRad9.1* sharply increased from unicellular pollen to bicellular pollen, and then maintained a high expression level, consistent with the fact that pollen was more sensitive to environmental factors [27, 28], whereas *OsRad9.2* continued its high-level expression over *OsRad9.1* (Figure 6A and C). If pollen (such as in the male sterile line m393LA) was aborted in the unicellular stage (Figure 6B), the expression pattern of *Rad9* was similar to that in roots instead of that in normally developed pollen (Figure 6A and C). These results suggested that the two *OsRad9* transcript isoforms played different roles in different developmental tissues.

3.4 Responses of *OsRad9* transcript isoforms to DNA genotoxic stresses

In response to DNA-damaging agents (UV, bleomycin, and MMC), *OsRad9* expression was promoted by UV, bleomycin, and MMC (Figure 7) similar to *hRad9* [26]. However, *OsRad9.1* expression increased faster with prolonged treatment time of genotoxicity compared with *OsRad9.2*. For example, expression of the former reached eight times over after 10 h of UV irradiation, whereas the response of *OsRad9.2* to UV irradiation was not sensitive (Figure 7A).

3.5 Induction of *OsRad9* transcript isoforms by environmental stresses

To assess the responses of *OsRad9* to environmental stresses, the expression of *OsRad9.1* and *OsRad9.2* was detected under stress conditions such as drought, salt, and heavy metals ($CdCl_2$ and $HgCl_2$). Results indicated that *OsRad9.1* and *OsRad9.2* expression was upregulated in all treatments (Figure 8), but the expression of *OsRad9.1* was much higher than that of *OsRad9.2*.

3.6 Expression patterns of *OsRad9* transcript isoforms response to auxin in the context of rice callus formation

ARF75 is recorded in the GenBank database; thus, *OsRad9* expression can be affected by the plant hormone auxin. For confirmation, we investigated the expression patterns of *OsRad9* transcript isoforms in the context of rice callus formation. Results showed that 2,4-D stimulated *Rad9* expression and that the expression trend of *OsRad9.1* was similar to that of *OsRad9.2*, i.e. the expression level increased with prolonged time (Figure 9A). However, the increase rate was much higher than that of *OsRad9.2*. At the optimum concentration 2 mg/L of 2,4-D, the expression level of *OsRad9.1* was 13 times (26/2) that of *OsRad9.2* (Figure 9A).

OsRad9.1 displayed different response patterns elicited by different species of growth hormones (Figure 9B). Short treatment times (24 h) with 2,4-D showed the

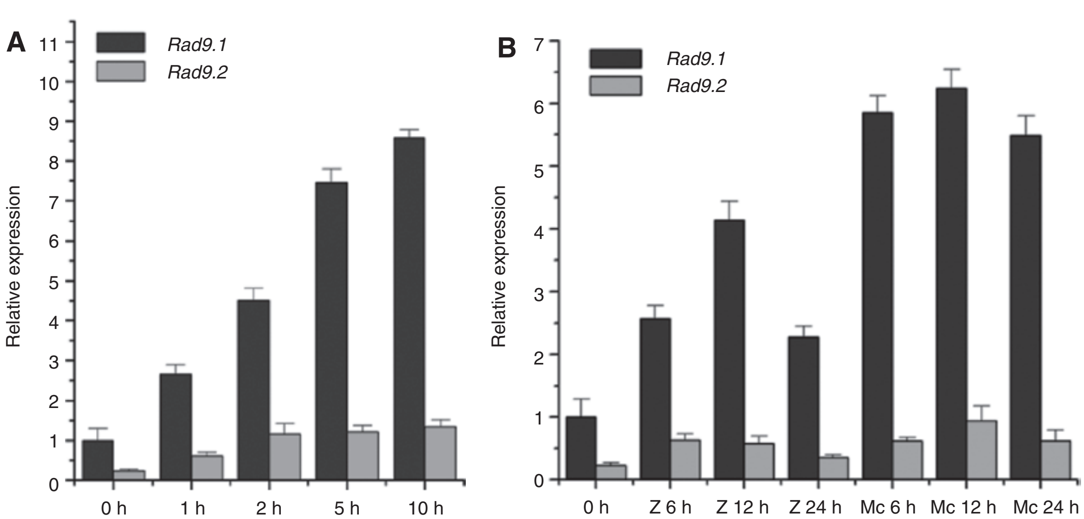

Figure 7: Transcript accumulation of *OsRad9* transcript isoforms in rice leaves in response to DNA genotoxic stresses as determined by qRT–PCR. Rice seedlings were treated with UV (A), bleomycin(z) and MMC(Mc) (B) at the indicated times.

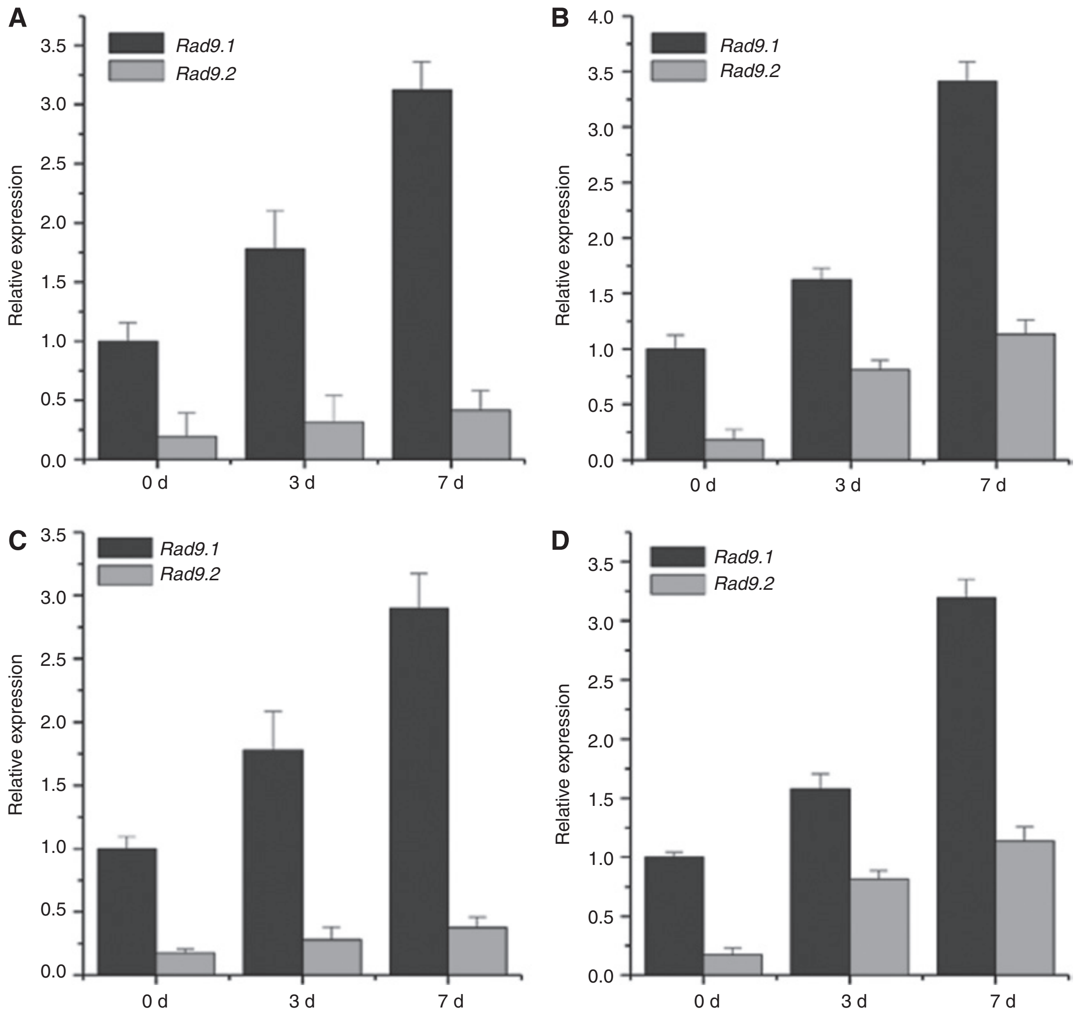

Figure 8: Transcript accumulation of *OsRad9* transcript isoforms in rice leaves in response to environmental stresses as determined by qRT–PCR. Rice seedlings were treated with drought (A), 0.2 M NaCl (B), 0.5 M $CdCl_2$ (C) and 0.5 M $HgCl_2$ (D) at the indicated times.

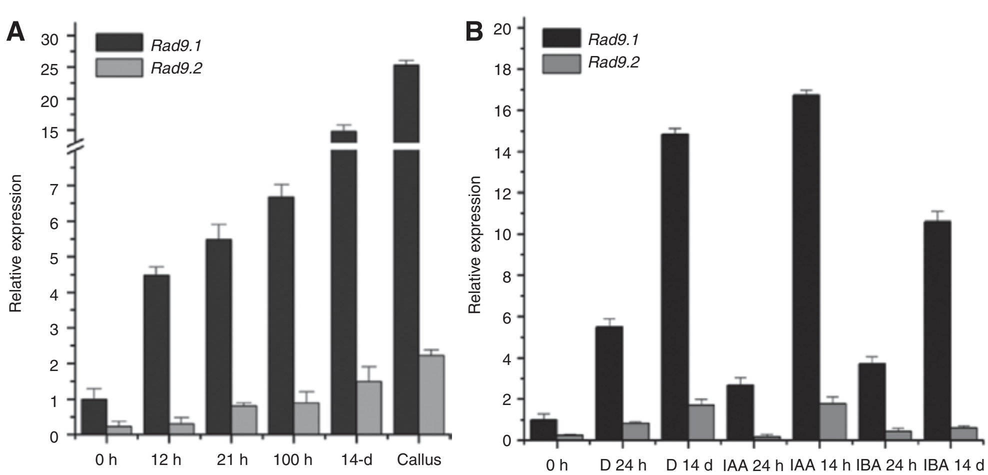

Figure 9: Expression patterns of *OsRad9* transcript isoforms response to auxin in the context of rice callus formation by qRT-PCR. (A) The effect of 2 mg/L 2,4-Dichlorophenoxyacetic acid (2, 4-D) on *OsRad9* transcript isoforms induction in the callus formation processes at different time points. (B) The effect of different auxins (2.0 mg/L 2, 4-D, IAA and IBA) on *OsRad9* transcript isoforms induction in calli at indicated times.

strongest effect in promoting *OsRad9* expression, whereas IAA showed the weakest. However, long-term treatment (14 days) with IAA intensively stimulated *OsRad9.1* expression rather than the opposite. As to *OsRad9.2*, the expression difference was not significant between IAA and 2,4-D (Figure 9B).

4 Discussion

In this paper, we identified and characterized *Rad9* of rice that is considered as *ARF75* deposited in GenBank. From the perspective of sequence structure, *OsRad9.1* and *OsRad9.2* (two protein isoforms of *OsRad9*) can function in the initial detection of DNA structural abnormalities by forming a 9-1-1 heterotrimeric complex with *Rad1* and *Hus1* [9]. However, from another point of view, *OsRad9.2* was strongly expressed in developmental pollen and weakly in somatic tissues and was not sensitive to genotoxic and other stress. Conversely, *OsRad9.1* was highly expressed in all tested tissues (Figures 6–9). The cell division of developmental pollen is known to be highly asymmetric, whereas that of somatic tissues is symmetric. *Rad9* is constitutively phosphorylated [9]. However, the role of *Rad9* phosphorylation in plant is unknown. Predictions from web-based KinasePhos servers showed that *OsRad9.2* lacks 9 phosphorylation sites, which are existed in the exon7 and exon8. Therefore, the differences between *OsRad9.1* and *OsRad9.2* in sequence structure and expression level indicated that the exon7 and exon8 of *OsRad9* likely contained some (x) factors to be studied in detail, which activated some undetermined pathway involved in the asymmetric division of pollen.

Meanwhile, many studies on plants, animals and yeasts have shown that environmental stresses such as salt, drought, and heavy metals induced the accumulation of reactive oxygen species (ROS) [29–31], which causes oxidative damage in DNA [32–34]. To counteract DNA damage, cells develop DNA damage responses. These responses sense DNA lesions and transmit the damage signal to activate the cell-cycle checkpoint control and thus delay cell cycle progression and repair the damaged DNA by recruiting the DNA repair machinery [35]. A comparison analysis of sequence structure and response of expression to stress factors such as drought, salt, heavy metals, and genotoxic agents showed that exon7 and exon8 made *OsRad9* insensitive to stress through mechanisms, whose details require further study.

Auxin is commonly used to plant tissue cultures and can significantly stimulate *OsRad9* expression (Figure 9), indicating that it is a bi-effect agent. On one hand, auxin promotes cell proliferation; on the other hand, it causes cell mutation or even death by DNA damage [36]. Based on a previous work, the auxin amount must be controlled in tissue culture depending on the research objective.

In summary, the rice cell-cycle checkpoint protein *OsRad9* gene identified in this paper was a bifunctional gene at the least. *OsRad9.1* was the basic processed product of *OsRad9* primary transcript mRNA (i.e. pre-mRNA) that participated in the cell cycle as a key component of DNA damage sensors and genotoxic stress response. Meanwhile, *OsRad9.2* was a splicing product of *OsRad9* pre-mRNA that is involved in the development of pollen.

Acknowledgments: We thank Dr. Haiqi Kang for providing rice male sterile line m393LA. This research was supported by the National Science Fund of China (No. 31070276 and No. 31270360).

References

1. Yoshiyama K, Sakaguchi K, Kimura S. DNA damage response in plants: conserved and variable response compared to animals. Biology 2013;2:1338–56.
2. Sancar A, Lindseyboltz LA, Unsalkaçmaz K, Linn S. Molecular mechanisms of mammalian dna repair and the dna damage checkpoints. Biochemistry 2004;73:39–85.
3. Stillman B. Cell cycle control of dna replication. Science 1996;274:1659–64.
4. Burtelow MA, Roos-Mattjus PM, Rauen M, Babendure JR, Karnitz LM. Reconstitution and molecular analysis of the hRad9-hHus1-hRad1 (9-1-1) DNA damage responsive checkpoint complex. J Biol Chem 2001;276:25903–9.
5. Xu M, Bai L, Gong Y, Xie W, Hang H, Jiang T. Structure and functional implications of the human Rad9-Hus1-Rad1 cell cycle checkpoint complex. J Biol Chem 2009;284:20457–61.
6. Alpi A. DNA damage checkpoint pathways and the maintenance of genome stability in C. elegans. Dissertation, 2004.
7. Warbrick E. PCNA binding through a conserved motif. Bioessays 1998;20:195–9.
8. Ueda S, Takeishi Y, Ohashi E, Tsurimoto T. Two serine phosphorylation sites in the C-terminus of Rad9 are critical for 9-1-1 binding to TopBP1 and activation of the DNA damage checkpoint response in hela cells. Genes Cells 2012;17:807–16.
9. Roos P, Hopkins KM, Oestreich AJ, Vroman BT, Johnson KL, Naylor S, et al. Phosphorylation of human Rad9 is required for Genotoxin-activated checkpoint signaling. J Biol Chem 2003;278:24428–37.
10. Rauen M, Burtelow MA, Dufault VM, Karnitz LM. The human checkpoint protein hRad17 interacts with the PCNA-like proteins hRad1, hHus1, and hRad9. J Biol Chem 2000;275:29767–71.
11. An L, Wang Y, Liu Y, Yang X, Liu C, Hu Z, et al. Rad9 is required for B cell proliferation and immunoglobulin class switch recombination. J Biol Chem 2010;285:35267–73.

12. Bessho T, Sancar A. Human DNA damage checkpoint protein hRAD9 is a 3′ to 5′ exonuclease. J Biol Chem 2000;275:7451–4.
13. Broustas CG, Lieberman HB. Contributions of rad9 to tumorigenesis. J Cell Biochem 2012;113:742–51.
14. Heitzeberg F, Chen I, Hartung F, Orel N, Angelis KJ, Puchta H. The rad17 homologue of arabidopsis is involved in the regulation of dna damage repair and homologous recombination. Plant J 2004;389:954–68.
15. Peng H, Chun J, Ai T, Tong Y, Zhang R, Zhao M, et al. MicroRNA profiles and their control of male gametophyte development in rice. Plant Mol Biol 2012;80:85–102.
16. Luo Y, Zhou H, Li Y, Chen J, Yang J, Chen Y, et al. Rice embryogenic calli express a unique set of microRNAs, suggesting regulatory roles of microRNAs in plant post-embryogenic development. FEBS Lett 2006;580:5111–6.
17. Wang W, Li R, Liu B, Li L, Wang S, Chen F. Alternatively spliced transcripts of group 3 late embryogenesis abundant protein from pogonatherum paniceum confer different abiotic stress tolerance in escherichia coli. J Plant Physiol 2012;169:1559–64.
18. Letunic I, Bork P. Interactive tree of life v2: online annotation and display of phylogenetic trees made easy. Nucleic Acids Res 2011;39:475–8.
19. Li F, Li M, Zhan C, Wang S. A reliable and high-efficiency agrobacterium tumefaciens-mediated transformation system of pogonatherum paniceum embryogenic callus using gfp as a reporter gene. Plant Cell, Tissue and Organ Culture (PCTOC). 2015;120:155–65.
20. Wang DK, Pei KM, Fu YP, Sun ZX, Li SJ, Liu HQ. Genome-wide analysis of the auxin response factors (ARF) gene family in rice (Oryza sativa). Gene 2007;394:13–24.
21. Roos P, Vroman BT, Burtelow MA, Rauen M, Eapen AK, Karnitz LM. Genotoxin-induced Rad9-Hus1-Rad1 (9-1-1) chromatin association is an early checkpoint signaling event. J Biol Chem 2002;277:43809–12.
22. Volkmer E, Karnitz LM. Human homologs of *schizosaccharomyces pombe* Rad1, hus1, and rad9 form a dna damage-responsive protein complex. J Biol Chem 1999;274:567–70.
23. Huang H, Lee T, Tzeng S, Horng J. KinasePhos: a Web Tool for Identifying Protein Kinase-specific Phosphorylation Sites. Nucleic Acids Res. 2005;33:226–9.
24. Kadir R, Bakhrat A, Tokarsky R, Abdu U. Localization of the drosophila rad9 protein to the nuclear membrane is regulated by the c-terminal region and is affected in the meiotic checkpoint. PLoS One 2012;7:617–22.
25. Lancelot N, Charier G, Couprie J, Duband I, Alpha B, Quémeneur E, et al. The checkpoint saccharomyces cerevisiae rad9 protein contains a tandem tudor domain that recognizes DNA. Nucleic Acids Res 2007;35:5898–912.
26. Burtelow MA, Kaufmann SH, Karnitz LM. Retention of the human rad9 checkpoint complex in extraction-resistant nuclear complexes after DNA damage. J Biol Chem 2000;275:26343–8.
27. Patterson BD, Mutton L, Paull RE, Nguyen VQ. Tomato pollen development: stages sensitive to chilling and a natural environment for the selection of resistant genotypes. Plant Cell Environ 1987;10:363–8.
28. Satake T, Koike S. Sterility caused by cooling treatment at the flowering stage in rice plants: I. The Stage and Organ Susceptible to Cool Temperature, Japanese J Corp Sci 1983;52:207–14.
29. Song J, Bent AF. Microbial pathogens trigger host DNA double-strand breaks whose abundance is reduced by plant defense responses. PLoS Pathogens 2014;10:151–65.
30. Biedermann S, Mooney S, Hellmann H. Recognition and repair pathways of damaged DNA in higher plants. selected topics in DNA repair. InTech 2011:477–83.
31. Wang R, Chen S, Zhou X, Shen X, Deng L, Zhu H, et al. Ionic homeostasis and reactive oxygen species control in leaves and xylem sap of two poplars subjected to NaCl stress. Tree Physiol 2008;28:947–57.
32. Guachalla LM, Rudolph KL. ROS induced DNA damage and checkpoint responses. Cell Cycle 2010;9:4058–60.
33. Burney S, Niles JC, Dedon PC, Tannenbaum SR. DNA damage in Deoxynucleosides and Oligonucleotides treated with Peroxynitrite. Chem Res Toxicol 1999;12:513–20.
34. Sharma P, Jha AB, Dubey RS, Pessarakli M. Reactive oxygen species, oxidative damage, and antioxidative defense mechanism in plants under stressful conditions. J Botany 2012;2012:1–26.
35. Ghosal G, Chen J. DNA damage tolerance: a double-edge sword guarding the genome. Transl Cancer Res 2013;3:107–29.
36. Dudits D, Ábrahám E, Miskolczi P, Ayaydin F, Bilgin M, Horváth GV. Cell-cycle control as a target for calcium, hormonal and developmental signals: the role of phosphorylation in the retinoblastoma-centred pathway. Ann Bot-London 2011;107:1193–202.